Development of Thermal Constriction Resistance for Anisotropic Rough Surfaces by the Method of Infinite Images

K. J. NEGUS*, M. M. YOVANOVICH† and J. W. DEVAAL*

Thermal Engineering Group
Department of Mechanical Engineering
University of Waterloo
Waterloo, Ontario

ABSTRACT

For many real contacting surfaces which possess anisotropic roughness, better predictions of the thermal contact resistance can be made by using an elemental heat flux tube consisting of an elliptical contact on a semi-infinite adiabatic rod of nominally rectangular cross-section. The constriction resistance of this elemental heat flux tube has been shown to be a perturbation of the half-space resistance for relatively small contact sizes. By combining the Surface Element Method and the novel Method of Infinite Images, useful approximate expressions for the two low-order perturbations have been developed.

The first-order perturbation is remarkably simple and independent of the contact shape, orientation and boundary condition. The second perturbation is much more complex. After comparing with limited previous data, the approximate expressions derived are expected to provide an adequate estimate of the constriction resistance of the complex three-dimensional elemental heat flux tube encountered with most practical problems of contacting anisotropic rough surfaces.

NOMENCLATURE

- a - semi-major axis length of elliptical contact
- A - area
- A_c - contact area
- A_t - nominal flux tube area, $A_t \equiv 4cd$
- b - semi-minor axis length of elliptical contact
- c - half-length of rectangular flux tube
- d - half-width of rectangular flux tube
- $f_1(\beta)$ - function of rectangle aspect ratio (Eqs.(33) or (36))
- $f_2(\beta)$ - function of rectangle aspect ratio (Eqs. (34) or (37))
- $F(\mu)$ - function of flux distribution (Eq. (53))
- $g(\beta)$ - function of rectangle aspect ratio (Eqs. (31) or (35))
- I - second moment of area or "moment of inertia"
- I_o - polar second moment of area about centroid of contact
- I_{RR} - radial second moment of area about axis joining centroids of starting and image sources
- k - homogeneous thermal conductivity
- $K(\cdot)$ - complete elliptic integral of the first kind
- L - arbitrary length into the flux tube
- N - number of image rows treated as discrete sources
- q - heat flux over contact
- q_e - effective heat flux outside region of discrete sources
- Q - total heat flux over contact
- r - polar coordinate
- R - distance between centroids of contacts
- R_c - thermal constriction resistance of elemental heat flux tube
- t - time heat flux has been applied to the contact
- T - temperature rise
- $\bar{T}$ - average temperature rise
- $\bar{T}_c$ - average temperature rise over contact
- $\bar{T}(z=L)$ - average temperature rise in flux tube plane $z=L$
- x,y - Cartesian coordinate system aligned with principal axes of contact distribution (see Fig. 2)
- z - Cartesian coordinate into depth of a half-space

Greek Symbols

- α - aspect ratio of elliptical contact, $\alpha \equiv b/a$
- α_o - homogeneous thermal diffusivity
- β - aspect ratio of nominally rectangular elemental heat flux tube, $\beta \equiv d/c$
- ε - dimensionless relative contact size, $\varepsilon \equiv (A_c/A_t)^{1/2}$
- $\zeta(\cdot)$ - Riemann's Zeta function
- η - local coordinate along semi-minor axis of elliptical contact
- θ - polar coordinate; angle between x-axis and axis joining starting and image sources

* Graduate Research Assistant
† Professor, Member ASME

Presented at the National Heat Transfer Conference
Denver, Colorado—August 4-7, 1985

μ - flux distribution parameter (μ=0 for uniform flux, μ= -1/2 for equivalent isothermal flux)

ξ - local coordinate along semi-major axis of elliptical contact

ρ - distance from point source of heat

ϕ - orientation angle of elliptical contact with respect to principal axis of contact distribution (see Fig. 2)

χ - argument of complete elliptic integral, $\chi \equiv (1 - \alpha^2)^{1/2}$

ψ - dimensionless thermal constriction resistance parameter, $\psi \equiv k\sqrt{A_c}\, R_c$

ψ_S - constriction parameter calculated by Sadhal (ref. [5])

ψ_{NYD} - constriction parameter calculated by approximate expressions derived in this work

Subscripts and Superscripts

A - refers to area contribution

c - refers to contact

ij - refers to location of image source (i,j) as shown in Fig. 2

I - refers to second moment of area or "inertia" contribution

rec - refers to uniform flux applied to a rectangle

si - refers to uniform flux applied over a semi-infinite body

x,y - refers to global Cartesian coordinate system

1,2 - refers to either contact 1 or 2 in Surface Element Method derivation

∞ - refers to half-space

ξ,η - refers to local coordinate system of elliptical contact

INTRODUCTION

Over the past twenty-five years a considerable research effort has uncovered much about the thermal resistance which occurs at the interface of contacting rough surfaces. Insight has been gained through the use of models which describe the surface topography and predict the contact geometry which results when two surfaces are forced together under a normal load. Once this contact geometry in known, thermal models describing how the heat flows through this geometry can be developed. In the best of these models to date [1,2], the constriction of heat is considered by evaluating the thermal resistance of a fundamental contact cell or elemental heat flux tube whose dimensions are determined from the average contact spot area and contact spot density over the interface. This thermal resistance is then used in generating the total interface resistance for the contacting surfaces.

When two rough surfaces are brought together under the assumptions of vacuum and negligible radiation across the gap, conduction of heat across the interface occurs through discrete regions of contact as illustrated in Fig. 1. The effects of an interstitial fluid and radiative heat transfer across the gap can be dealt with separately if necessary. Determining the conduction resistance across the interface obviously requires knowledge about the geometry of the individual heat flow paths spanning the contact interface.

For contact between two generally anisotropic surfaces, predicting the exact shapes, distribution and sizes of contact regions is a formidable task. Fortunately, as shown for isotropic surfaces, specific information about individual contact spots

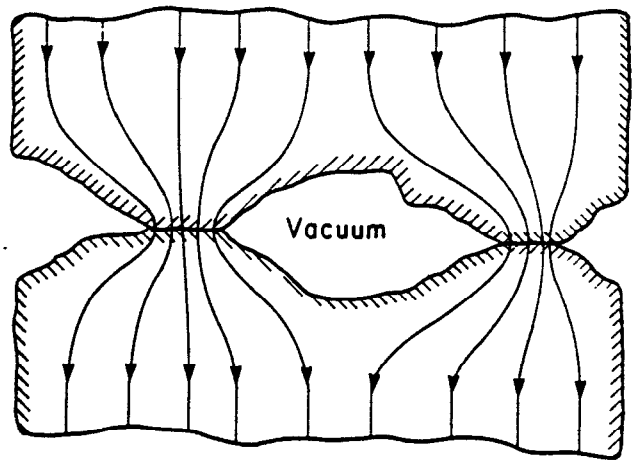

Fig. 1 Constriction of heat flow between contacting rough surfaces

is not critical in determining the contact resistance of the interface. If the contact interface is repetitive, due to both uniform surface roughness and global conformity of the surfaces, a certain uniformity will develop in the individual heat flow paths spanning the interface which allows the total interface behaviour to be characterized by the thermal behaviour of the average heat flow path.

Grinding, turning, and milling are all processes known to produce uniform surface finishes which, in general, have much higher slopes across the cutting direction than parallel to it. Another distinctive feature of these anisotropic surfaces is the existence of dominant frequency components in the spectral analysis of profilometer traces taken across the cutting direction [3]. These dominant frequency components generally correspond to the cutting tool crossfeed or to either workpiece or tool vibration during machining. Contact between two such surfaces at some arbitrary angle produces a rectangular array of elliptical contact spots as shown in Fig. 2. Once the contact area has been found by elastic or plastic deformation analysis, the aspect ratio and orientation of the contact ellipses can be determined from the geometric intersection of the individual surfaces at the contact locations. Contact spot size, aspect ratio, orientation and spacing over the contact interface are then all used to determine the dimensions of the individual elemental heat flux tube as illustrated in Fig. 3.

When more sophisticated stochastic models are chosen to describe the surfaces, the determination of the dimensions for the elemental heat flux tube becomes much more complicated but the essential geometry remains unchanged. An example is the two-dimensional, random, Gaussian surface model developed by Longuet-Higgins [4] in 1956.

For the anisotropic contact model as shown in Fig. 3, the adiabatic surface of the elemental flux tube is rectangular far into the depth. Near the contact surface though, a slight deviation occurs because the contacts residing immediately next to the contact of interest are not completely symmetric about rectangular sides. If the principal axes of the ellipse and rectangle coincide, then an analytic solution exists in the form of a slowly convergent double-infinite Fourier series [5]. The general problem might be solvable by a numerical technique such as finite elements or finite volumes. However the heat flow is fully three-dimensional and thus a numerical solution would require a major commitment of time, effort and computational resources.

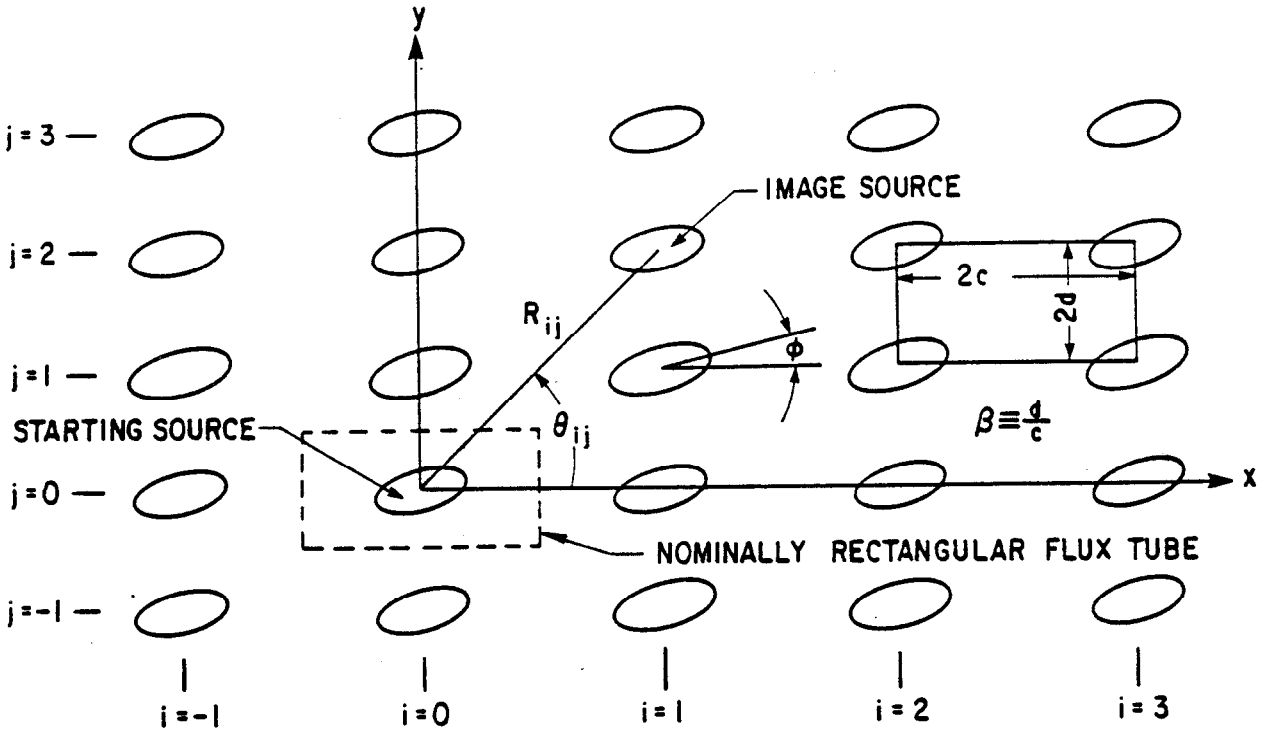

Fig. 2 Arrangement of starting and image sources

An approximate solution valid over a range encompassing most contact resistance problems can be developed by actually treating the more complex problem of the elliptical contact on the slightly non-rectangular flux tube. The basis of this approximate solution comes from the concept of superposing the temperature rise due to a single elliptical contact on a half-space with the temperature rises due to an "infinite" number of similar elliptical "images". This method has been utilized previously [6] for the simpler problem of circular contacts on square flux tubes.

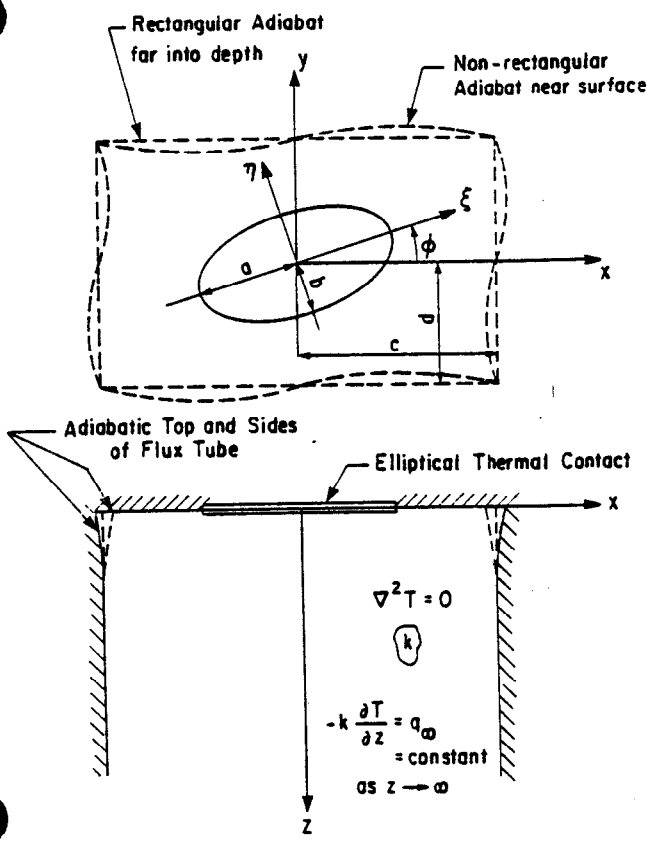

Fig. 3 Nominally rectangular elemental heat flux tube

Ideally the boundary condition over the contact of Fig. 3 would be that of an isotherm. However this creates a mixed boundary value problem which is difficult to treat analytically. Fortunately excellent results can be obtained for the thermal constriction resistance by assuming a specified flux over the contact of the form

$$q = q_o\left[1 - \left(\frac{\xi}{a}\right)^2 - \left(\frac{\eta}{b}\right)^2\right]^\mu \qquad (1)$$

The cases of immediate interest are $\mu=0$, the uniform flux, and $\mu=-1/2$, the equivalent isothermal flux. Previous experience shows that these two cases provide upper and lower bounds respectively to the expected resistance. The equivalent isothermal flux is in fact the contact flux which results from an isothermal elliptical contact on an adiabatic half-space. A method to combine the results from flux specified contacts to approximate the true mixed boundary value problem is described in [7] but will not be used in this work.

DERIVATION OF CONSTRICTION RESISTANCE BY METHOD OF INFINITE IMAGES

To derive the constriction resistance for the unit cell or elemental heat flux tube of Fig. 3, the temperature fields due to an infinite number of elliptical thermal contacts on an adiabatic half-space will be linearly superposed. As shown in Fig. 2 one of the contacts will be labeled as the "starting source" while all others are then the "image sources". This solution technique will be called the Method of Infinite Images since the number of image sources will be arbitrarily large.

By linear superposition the average temperature rise on the starting contact, $\bar{T}_c$, can be written as

$$\bar{T}_c = \bar{T}_\infty + \sum_{i=-\infty}^{\infty} \sum_{j=-\infty}^{\infty} \bar{T}_{ij} \qquad (2)$$

where $\bar{T}_\infty$ is the average temperature rise due to the starting source alone on an adiabatic half-space and $\bar{T}_{ij}$ is the average induced temperature rise on the starting source due to the image source (i,j).

The average induced temperature rise $\bar{T}_{ij}$ can be estimated by the Surface Element Method [8] for steady-state conditions. From the derivation in Appendix I of this work, an approximate expression for $\bar{T}_{ij}$ is

$$\bar{T}_{ij} = \frac{q}{2\pi k}\left\{\frac{A_c}{R_{ij}} + \frac{2I_o - 3I_{RR}^{ij}}{R_{ij}^3}\right\} \qquad (3)$$

where q is the uniform heat flux over the image source, k the homogeneous thermal conductivity, A_c the contact area of both the starting and image sources, I_o the polar second moment of area about the centroid of the contact, I_{RR}^{ij} the radial second moment of area about the axis joining the starting and image sources, and R_{ij} the distance between the centroids of the starting and image sources, or

$$R_{ij} = 2[(ic)^2 + (jd)^2]^{1/2} \qquad (4)$$

Note that Eq.(3) assumes that a uniform heat flux is applied to all contacts. Thus the following derivation is made for the uniform flux case specifically. However it will be shown later that the resultant expression for the constriction resistance can be easily extended to the other contact flux case of interest.

The approximate expression for $\bar{T}_{ij}$ contains an "area" term and an "inertia" term (or "second moment of area" term). Thus $\bar{T}_c$ can also be written as

$$\bar{T}_c = \bar{T}_\infty + \bar{T}^A + \bar{T}^I \qquad (5)$$

where $\bar{T}^A$ and $\bar{T}^I$ represent the "area" and "inertia" contributions to $\bar{T}_c$ due to all the image sources.

The fact that a true steady-state condition does not exist for a truly infinite number of contacts must be acknowledged to evaluate $\bar{T}^A$. That is, for any length of time thre will always be some image contacts so far from the starting source that their induced temperature rises are not yet steady. Thus only N rows or columns of images will be treated as discrete sources. As shown in Fig. 4, outside the rectangular region where the image sources are discrete, the induced-effect temperature rise contribution to $\bar{T}_c$ will be given approximately by a uniform effective flux q_e over the remainder of the surface of the half-space. The area term can be written as

$$\bar{T}^A = \bar{T}^A_{xx} + \bar{T}^A_{yy} + \bar{T}^A_{xy} + \bar{T}^A_{si} + \bar{T}^A_{rec} \qquad (6)$$

The terms $\bar{T}^A_{xx}$, $\bar{T}^A_{yy}$ and $\bar{T}^A_{xy}$ represent the contributions to $\bar{T}^A$ due to the discrete sources and are given by

$$\bar{T}_{xx} = \frac{qA_c}{2\pi kc} \sum_{i=1}^{N} \frac{1}{i} \qquad (7)$$

$$\bar{T}_{yy} = \frac{qA_c}{2\pi kd} \sum_{j=1}^{N} \frac{1}{j} \qquad (8)$$

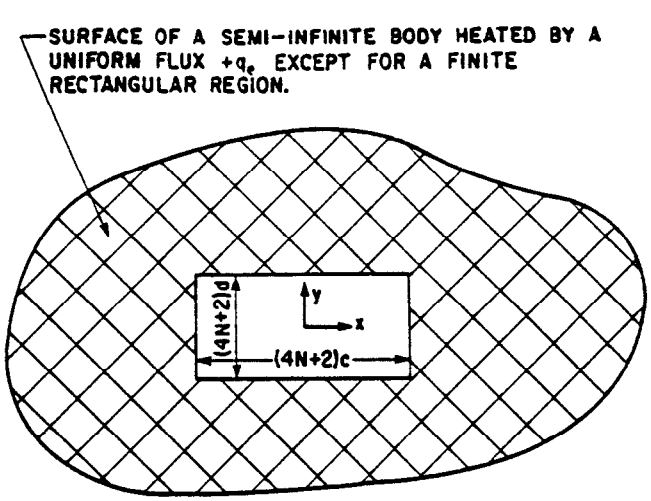

Fig. 4 Uniform effective flux heating of surface outside region of discrete sources

$$\bar{T}_{xy} = \frac{qA_c}{\pi kc} \sum_{i=1}^{N} \sum_{j=1}^{N} (i^2 + \beta^2 j^2)^{-1/2} \qquad (9)$$

where $\beta \equiv d/c$ is the aspect ratio of the nominally rectangular heat flux tube.

For the contribution to $\bar{T}^A$ from sources outside the finite rectangular region of Fig. 4, consider first the temperature rise on the surface of a semi-infinite body with uniform flux q_e[9]:

$$\bar{T}^A_{si} = \frac{2q_e}{k}\left[\frac{\alpha_o t}{\pi}\right]^{1/2} \qquad (10)$$

where α_o is the homogeneous thermal diffusivity, t the elapsed time that the flux has been applied, and q_e is the effective uniform flux given by

$$q_e = q\, A_c/4cd \qquad (11)$$

However for the finite rectangular region of discrete sources this uniform flux has not been applied. Thus the temperature rise due to a flux $-q_e$ over a rectangular region must be superposed to give the correct temperature contribution from the finite number of image sources treated as a uniform effective flux. From [10] this temperature rise is

$$\bar{T}^A_{rec} = -\frac{2}{\pi}\frac{q_e}{k}\left\{(2N+1)c\ \ln\tan\left[\frac{\pi}{4} + \frac{1}{2}\tan^{-1}\beta\right] + (2N+1)d\ \ln\tan\left[\frac{\pi}{4} + \frac{1}{2}\tan^{-1}\frac{1}{\beta}\right]\right\} \qquad (12)$$

Note that this is really the temperature rise at the centroid of the starting source due to a rectangular contact region (2N+1)d x (2N+1)c with uniform flux $-q_e$. In this work the average temperature rise over the starting contact is required. Fortunately the average temperature rise contribution is nearly the same as this value and in the limit as N becomes arbitrarily large they will be identical.

To summarize then, an approximate expression for the induced average temperature rise on the starting source due to "area" terms in $\bar{T}_{ij}$ is given by

$$\bar{T}^A = \frac{qA_c}{2\pi kc}\left\{\left(1 + \frac{1}{\beta}\right)\sum_{i=1}^{N}\frac{1}{i} + 2\sum_{i=1}^{N}\sum_{j=1}^{N}(i^2+\beta^2 j^2)^{-1/2} + \frac{1}{d}[\pi\alpha_o t]^{1/2} - \frac{(2N+1)}{\beta}\left[\ln\tan\left(\frac{\pi}{4} + \frac{1}{2}\tan^{-1}\beta\right) + \beta\ \ln\tan\left(\frac{\pi}{4} + \frac{1}{2}\tan^{-1}\frac{1}{\beta}\right)\right]\right\} \qquad (13)$$

The "inertia" term contribution to the average temperature rise on the starting source can be written as

$$\bar{T}^I = \bar{T}^I_{xx} + \bar{T}^I_{yy} + \bar{T}^I_{xy13} + \bar{T}^I_{xy24} \tag{14}$$

The first term represents the contribution from the discrete sources on the x-axis or

$$\bar{T}^I_{xx} = 2\left\{ \frac{q}{2\pi k} \sum_{i=1}^{N} \frac{2I_o - 3I^{io}_{RR}}{R^3_{io}} \right\} \tag{15}$$

where for all cases

$$I_o \equiv I_{xx} + I_{yy} \tag{16}$$

and for the x-axis $I^{io}_{RR} = I_{xx}$. I_{xx} and I_{yy} are the second moments of area of the contact about the principal axes x and y of the contact distribution as shown in Fig. 5. Thus

$$\bar{T}^I_{xx} = \frac{q}{8\pi kc^3}(2I_{yy} - I_{xx}) \sum_{i=1}^{N} \frac{1}{i^3} \tag{17}$$

and similarly

$$\bar{T}^I_{yy} = \frac{q}{8\pi kd^3}(2I_{xx} - I_{yy}) \sum_{j=1}^{N} \frac{1}{j^3} \tag{18}$$

The contributions to $\bar{T}^I$ due to the discrete image sources not located on the x-y axes are identical for quadrants I and III and for quadrants II and IV. Thus

$$\bar{T}^I_{xy13} = 2\left\{\frac{q}{2\pi k} \sum_{i=1}^{N} \sum_{j=1}^{N} \frac{2I_o - 3I^{ij}_{RR}}{R^3_{ij}} \right\}$$

$$= \frac{q}{8\pi kc^3} \sum_{i=1}^{N} \sum_{j=1}^{N} (i^2+\beta^2 j^2)^{-3/2}(2I_o - 3I^{ij}_{RR}) \tag{19}$$

where for quadrants I and III [11]

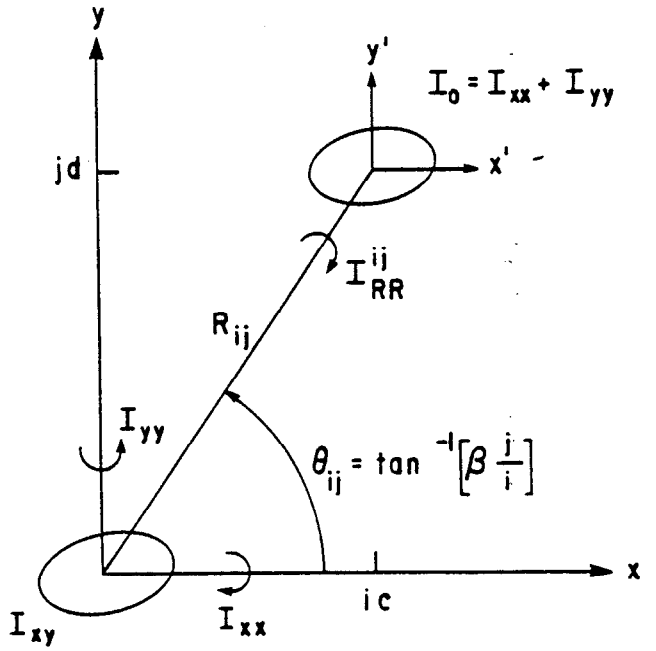

Fig. 5 Second moments of area for image and starting sources

$$I^{ij}_{RR} = I_{xx}\cos^2\theta_{ij} + I_{yy}\sin^2\theta_{ij} + 2I_{xy}\sin\theta_{ij}\cos\theta_{ij} \tag{20}$$

and as shown in Fig. 5

$$\theta_{ij} = \tan^{-1}(\beta \frac{j}{i}) \tag{21}$$

Similarly for quadrants II and IV

$$\bar{T}^I_{xy24} = \frac{q}{8\pi kc^3} \sum_{i=1}^{N} \sum_{j=1}^{N} (i^2+\beta^2 j^2)^{-3/2}(2I_o - 3I^{ij}_{RR}) \tag{22}$$

where

$$I^{ij}_{RR} = I_{xx}\cos^2\theta_{ij} + I_{yy}\sin^2\theta_{ij} - 2I_{xy}\sin\theta_{ij}\cos\theta_{ij} \tag{23}$$

Thus the average temperature rise contribution due to the inertia terms can be written as

$$\bar{T}^I = \frac{q}{8\pi kc^3}\left\{[(2I_{yy} - I_{xx}) + \frac{1}{\beta^3}(2I_{xx} - I_{yy})] \sum_{i=1}^{N} \frac{1}{i^3} + 2[2I_{yy} - I_{xx}] \sum_{i=1}^{N} \sum_{j=1}^{N} (i^2 + \beta^2 j^2)^{-3/2} + 6[I_{xx} - I_{yy}] \sum_{i=1}^{N} \sum_{j=1}^{N} (i^2+\beta^2 j^2)^{-3/2}\sin^2\theta_{ij}\right\} \tag{24}$$

An approximate expression for the average temperature rise for the starting contact on an elemental heat flux tube of semi-infinite length is then given by combining Eqs. (5), (13) and (24). From Eq. (13) it is obvious that for a contact area supplying a heat flux to a semi-infinite flux tube, a steady-steady contact temperature will never be reached. However in reality a quasi-steady value of the constriction resistance is obtained in only several milliseconds for most surfaces [12]. In fact elemental heat flux tubes of only finite length can define the constriction resistance which is the parameter of interest in this work. As shown in [13] all constriction resistance for a circular contact on a circular flux tube was accounted for with a flux tube length equal to the flux tube radius and in this case a steady-state contact temperature would exist. However, by allowing the number of image contacts to become arbitrarily large, relatively simple expressions can be developed for all ranges of the parameters involved.

A common definition of the constriction resistance, R_c, is

$$R_c = \frac{\bar{T}_c - \bar{T}(z=L)}{Q} = \frac{L}{kA_t} \tag{25}$$

where $\bar{T}_c$ is the average contact temperature rise, $\bar{T}(z=L)$ the average temperature rise in some plane z=L of the elemental flux tube, Q the total heat flux in the tube and A_t the nominal cross-sectional area of the flux tube. Conceptually the constriction resistance is the total resistance between two planes of the flux tube minus the resistance due solely to one-dimensional heat conduction.

After a sufficiently long time t and for a large length L, one can approximate $\bar{T}(z=L)$ as being due to a uniform effective flux q_e applied over the surface of a semi-infinite body, or from [6]

$$\overline{T}(z=L) = \frac{qA_c}{2\pi kcd}\,[\pi\alpha_o t]^{1/2} - \frac{qA_c L}{4kcd} \qquad (26)$$

Since $Q = qA_c$ and $A_t = 4cd$ then

$$R_c = \frac{\overline{T}_c}{qA_c} = \frac{[\pi\alpha_o t]^{1/2}}{2\pi kcd} \qquad (27)$$

A dimensionless thermal constriction resistance parameter will now be defined as

$$\psi \equiv k\sqrt{A_c}\,R_c \qquad (28)$$

where $\sqrt{A_c}$ has been chosen to non-dimensionalize R_c because both previous experience [14] and analytical considerations [15] have shown this quantity to be the characteristic dimension of length for constriction problems.

To complete the derivation the number of images treated as discrete sources will be allowed to become arbitrarily large and a dimensionless relative contact size will be defined as

$$\varepsilon \equiv (A_c/A_t)^{1/2} \qquad (29)$$

The constriction parameter then becomes

$$\psi = \psi_\infty + \varepsilon g(\beta) + \frac{\varepsilon^3\beta^{3/2}}{\pi A_c^2}\{[(2I_{yy} - I_{xx}) + \frac{1}{\beta^3}(2I_{xx} - I_{yy})]f_o + 2[2I_{yy} - I_{xx}]f_1(\beta) + 6[I_{xx} - I_{yy}]f_2(\beta)\} \qquad (30)$$

where ψ_∞ is the dimensionless constriction resistance of the starting source on an adiabatic half-space and

$$g(\beta) \equiv \frac{\sqrt{\beta}}{\pi}\lim_{N\to\infty}\{(1+\frac{1}{\beta})\sum_{i=1}^{N}\frac{1}{i} + 2\sum_{i=1}^{N}\sum_{j=1}^{N}(i^2+\beta^2j^2)^{-1/2} - \frac{(2N+1)}{\beta}[\ln\tan(\frac{\pi}{4}+\frac{1}{2}\tan^{-1}\beta) + \beta\ln\tan(\frac{\pi}{4}+\frac{1}{2}\tan^{-1}\frac{1}{\beta})]\} \qquad (31)$$

$$f_o \equiv \sum_{i=1}^{\infty}\frac{1}{i^3} = \zeta(3) \approx 1.2021 \qquad (32)$$

$$f_1(\beta) \equiv \sum_{i=1}^{\infty}\sum_{j=1}^{\infty}(i^2+\beta^2j^2)^{-3/2} \qquad (33)$$

$$f_2(\beta) \equiv \sum_{i=1}^{\infty}\sum_{j=1}^{\infty}(i^2+\beta^2j^2)^{-3/2}\sin^2\theta_{ij} \qquad (34)$$

where $\zeta(\cdot)$ is Riemann's Zeta Function [16].

Although elliptical contacts have appeared in all illustrations, the preceding approximate expression for the constriction parameter is valid for any arbitrary contact area with uniform flux on a nominally rectangular flux tube. To use Eq.(30) effectively for the problem of interest, an elliptical contact resulting from anisotropic roughness, the following tasks must be performed:

i) Development of useful approximate expressions for $g(\beta)$, $f_1(\beta)$ and $f_2(\beta)$.
ii) Extension of Eq.(30) for the equivalent isothermal flux distribution.
iii) Development of expressions for the half-space resistance for both flux cases.
iv) Development of expressions for I_{xx} and I_{yy} for the case of an elliptical contact orientated at an angle ϕ with respect to the principal axes of the contact distribution as shown in Fig. 2.

Approximate Expressions for $g(\beta)$, $f_1(\beta)$ and $f_2(\beta)$

To develop approximate expressions for $g(\beta)$, $f_1(\beta)$ and $f_2(\beta)$, accurate values of these functions were generated over a wide range of β. Most of the test values were from the range $0.1 \le \beta \le 1$ which should encompass most practical problems from anisotropic roughness. However to be thorough some values of β as low as .001 were also calculated. In [6] a simple method for extrapolating a converged result from finite summations was given and this method was used for the results to follow. In Figs. 6 and 7 the most accurate values for $g(\beta)$, $f_1(\beta)$ and $f_2(\beta)$ are shown graphically. The computations were performed in double precision BASIC on an IBM-PC.

To avoid lengthy summations, simple correlations have been made using a non-linear, least squares algorithm [17] written in BASIC for the IBM-PC. These correlations give

$$g(\beta) = .691\,\beta^{-.640} - 1.313 + .430\ln\beta - .0683(\ln\beta)^2 \qquad (35)$$

$$f_1(\beta) = \frac{1.65}{\beta} - e^{-\frac{.00360}{\beta}}[.646 - .051\beta] \qquad (36)$$

$$f_2(\beta) = \frac{.560}{\beta} - .095 + .222\,\beta - .160\,\beta^2 \qquad (37)$$

These correlations are all valid over the range $.001 \le \beta \le 1$ and all have maximum relative errors of less than 1% with respect to their input data.

The behaviour of the function $g(\beta)$ has an important physical interpretation. The ratio of real contact area to total surface area is typically much less than 1% or $\varepsilon \equiv \sqrt{A_c/A_t} < .1$ for most practical problems where contact resistance is significant. In this case a good approximation to the dimensionless constriction parameter is

$$\psi = \psi_\infty + g(\beta)\varepsilon \qquad (38)$$

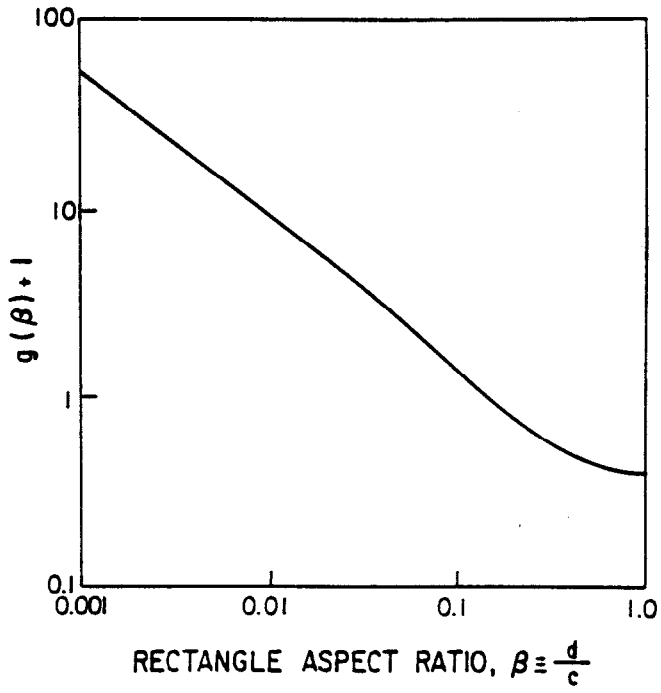

Fig. 6 Function $g(\beta)$ versus rectangle aspect ratio β

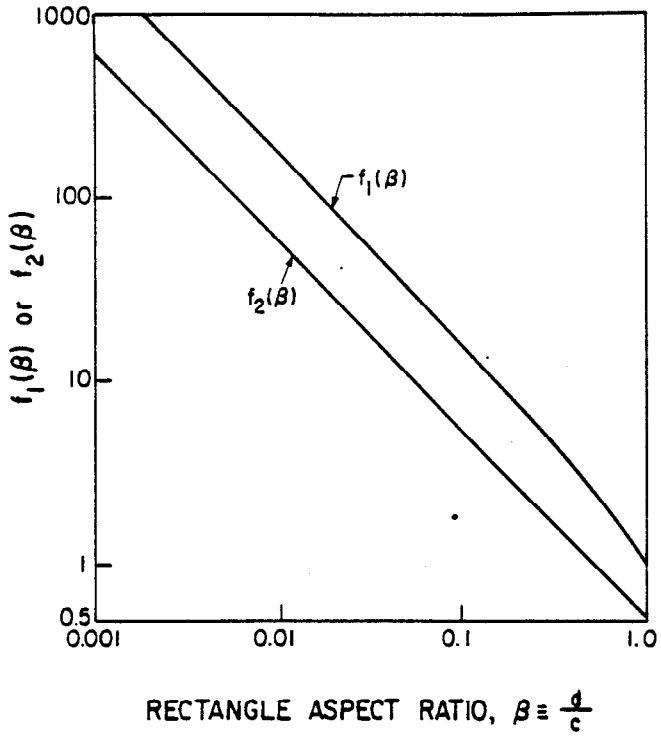

Fig. 7 Functions $f_1(\beta)$ and $f_2(\beta)$ versus rectangle aspect ratio β

As shown graphically in Fig. 6, $g(\beta)$ has a value of $-.621$ at $\beta=1$. It then becomes less negative with decreasing β, reaches a value of zero around $\beta \approx .14$, and then becomes positive and approximately proportional to $\beta^{-3/4}$. Thus if the contact aspect ratio is fixed (ψ_∞ = constant) and the relative contact size ε is constant, then decreasing β will cause an increase in the contact resistance. Furthermore, for $\beta<.14$ the constriction parameter for the elemental flux tube is actually higher than that of a contact on a half-space which was previously considered an upper bound. A simple physical justification for these results would be that at very small values of β the constant areas located parallel to the y-axis of Fig. 2 begin to behave collectively as strip contacts which are generally more resistive per unit area than discrete contacts.

Extension to Case of Equivalent Isothermal Flux

As mentioned previously the exact boundary condition for each elliptical contact is close to that of an isotherm. However this creates a mixed boundary value problem which is exceedingly difficult to handle analytically. Fortunately the problem can be avoided by prescribing flux distributions over the contact and determining a resistance based on the average contact temperature. Previous experience has also shown that the uniform flux and equivalent isothermal flux distributions provide upper and lower bounds on the expected resistance of the physical system. The equivalent isothermal flux distribution is defined as the contact flux which results from an isothermal contact on an adiabatic half-space, or for an ellipse

$$q = q_o\left[1 - \left(\frac{\xi}{a}\right)^2 - \left(\frac{\eta}{b}\right)^2\right]^{-1/2} \qquad (39)$$

where ξ-η is a local coordinate system along the major and minor axes of the ellipse as shown in Fig. 3. Note that the resistance calculated from this prescribed flux is nearly identical to that obtained from an isothermal contact when the elliptical contact area is much smaller than the cross-sectional area of the elemental flux tube ($\varepsilon<.3$).

The expressions developed in this work to approximate the constriction resistance have so far assumed a uniform flux distribution over an elliptical contact. The approximate constriction parameter expression can be written conceptually as

$$\psi = \psi_\infty + \varepsilon\psi_A + \varepsilon^3\,\psi_I \qquad (40)$$

To use this expression for the equivalent isothermal flux case, each term in this expression must be examined separately.

The first term, ψ_∞, is the dimensionless resistance of the contact on an adiabatic half-space. With the equivalent isothermal flux this parameter is slightly different than for the uniform flux but nonetheless readily available. Since ψ_∞ is also dependent on the ellipse aspect ratio then in functional form

$$\psi_\infty = \psi_\infty(\alpha,\mu) \qquad (41)$$

where $\alpha\equiv b/a$ is the aspect ratio of the ellipse and μ is the flux distribution parameter from Eq. (1) ($\mu=0$ for the uniform flux and $\mu=-1/2$ for the equivalent isothermal flux).

To understand the effect of flux distribution on the second term ψ_A, the origin of this term from its integral form in Appendix I must be considered. For a non-uniform flux distribution this term is proportional to

$$\psi_A \propto \left[\int_A q\,dA\right]/Q \qquad (42)$$

where Q is the total heat flux over the contact. Obviously since Q is given by

$$Q = \int_A q\,dA \qquad (43)$$

then the term ψ_A will be the same for any flux distribution over the contact. In functional form then

$$\psi_A = \psi_A(\beta) \qquad (44)$$

where $\beta\equiv d/c$ is the aspect ratio of the nominally rectangular elemental heat flux tube.

It is of paramount importance to note the existence of a second integral which vanishes for a uniform flux distribution. From Appendix I this integral is

$$I = \int_A q\,r\cos\theta\,dA \qquad (45)$$

where r-θ is a local coordinate system about the centroid of the contact. If q is either constant or symmetric about both the centroid and any axis through the centroid, then I vanishes by the definition of centroidal location. Fortunately the equivalent isothermal flux on an elliptical contact meets the second criterion and as with the uniform flux this term is identically zero (ie. no ε^2 - term). One can also show that all the ε^2, ε^4, ε^6, ...-terms vanish as well for such symmetric flux distributions.

The final term in the approximate expression, ψ_I, is given by the third integral term in Appendix I which gives rise to the polar and radial second moments of area (or "moments of inertia") I_o and I_{RR}. If a non-uniform flux is applied over the contact then some change will result to this term.

Since this term will also be a function of the aspect ratios of both the ellipse and nominally rectangular flux tube and the orientation angle of the elliptical contact ϕ as shown in Fig. 2, then in functional form

$$\psi_I = \psi_I (\alpha, \beta, \phi, \mu) \tag{46}$$

In this work the dependence on μ will be ignored for two reasons. First a rough calculation for the limiting case of a circular contact shows that the difference in ψ_I for $\mu=0$ and $\mu=-1/2$ is about 15%. Since the $\psi_I\varepsilon^3$ term seldom contributes more than 5% (and often less than 1%) to the final result for the practical applications envisioned, neglecting μ in ψ_I should not cause significant error. The second reason is that in the case of large ε where the term $\psi_I\varepsilon^3$ contributes significantly to the final result, the absence of the ε^5-term will probably cause much greater error than neglecting the μ-dependence in ψ_I.

Thus in summary the constriction parameter for the elemental heat flux tube is a function of five parameters and is given by the approximation

$$\psi = \psi(\alpha, \beta, \varepsilon, \phi, \mu)$$
$$= \psi_\infty(\alpha, \mu) + \varepsilon\, \psi_A(\beta) + \varepsilon^3\, \psi_I (\alpha, \beta, \phi) \tag{47}$$

Half-Space Constriction Parameters

For an elliptical contact on an adiabatic half-space with an equivalent isothermal flux, the constriction resistance is given by [18] as

$$R_c = \frac{K(\chi)}{2\pi ak} \tag{48}$$

where $\chi \equiv \sqrt{1-\alpha^2}$. $K(\cdot)$ is the complete elliptic integral of the first kind and $a \geq b$ or $\alpha \leq 1$. Thus for the $\mu=-1/2$ flux distribution the half-space constriction parameter is

$$\psi_\infty (\alpha, \mu=-1/2) = \frac{1}{2} \left(\frac{\alpha}{\pi}\right)^{1/2} K(\chi) \tag{49}$$

Although a rigorous proof will not be presented in this work, it can be shown [19] that the constriction parameter for the uniform flux case differs from that of the equivalent isothermal flux by only a constant factor of $8/3\pi^2 = 1.0808$. Thus the constriction parameter for the uniform flux case is

$$\psi_\infty (\alpha, \mu=0) = \frac{8}{3\pi^2}\, \psi_\infty (\alpha, \mu=-1/2) \tag{50}$$

The complete elliptic integral $K(\chi)$ can also be approximated by simple expressions in terms of α with acceptable accuracy. With two approximations for two different ranges of α

$$\psi_\infty(\alpha,\mu) \approx F(\mu)\, \frac{\sqrt{\pi\alpha}}{(1+\sqrt{\alpha})^2} \qquad .2 \leq \alpha \leq 1 \tag{51}$$

$$\psi_\infty(\alpha,\mu) \approx F(\mu)\, \frac{1}{2}\left(\frac{\alpha}{\pi}\right)^{1/2} \left[\ln\left(\frac{4}{\alpha}\right) + \frac{\alpha^2}{4}\left(\ln\left(\frac{4}{\alpha}\right) - 2\right)\right] \qquad \alpha \leq .2 \tag{52}$$

where

$$F(\mu) = \begin{cases} \dfrac{8}{3\pi^2}, & \mu = 0 \\ 1, & \mu = -1/2 \end{cases} \tag{53}$$

These approximations can be derived from Theta functions for $.2 \leq \alpha \leq 1$ [20,21] and from a power series for $\alpha \leq .2$ [20]. The maximum error encountered in $\psi_\infty(\alpha, \mu)$ using the above approximations is about .5% at $\alpha=.2$.

Second Moments of Area for an Elliptical Contact

The orientation of an elliptical contact with respect to the principal axes of the contact distribution is shown in Fig. 8. The approximate expression derived for the constriction parameter of the elemental heat flux tube requires the second moments of area I_{xx} and I_{yy}. From [11] it can be shown

$$I_{xx} = I_{\xi\xi} \cos\phi^2 + I_{\eta\eta}\sin^2\phi - 2I_{\xi\eta}\cos\phi \sin\phi \tag{54}$$

where second moments of area, $I_{\xi\xi}$, $I_{\eta\eta}$ and $I_{\xi\eta}$ are with respect to the local coordinate system ξ-η. These quantities are [22]

$$I_{\xi\xi} = \frac{\pi}{4} ab^3 \tag{55}$$

$$I_{\eta\eta} = \frac{\pi}{4} a^3 b \tag{56}$$

$$I_{\xi\eta} = 0 \tag{57}$$

Thus the second moments of area required in Eq. (30) for the approximate constriction parameter are given by

$$I_{xx} = \frac{\pi ab}{4} (b^2\cos^2\phi + a^2\sin^2\phi) \tag{58}$$

$$I_{yy} = \frac{\pi ab}{4} (b^2\sin^2\phi + a^2\cos^2\phi) \tag{59}$$

APPROXIMATE EXPRESSION FOR CONSTRICTION PARAMETER

In the preceding sections approximate or exact expressions have been developed for $\psi_\infty(\alpha, \mu)$, $g(\beta)$, $f_1(\beta)$, $f_2(\beta)$, I_{xx} and I_{yy}. By combining these expressions, the approximate dimensionless constriction parameter for an elliptical contact on the elemental heat flux tube for anisotropic rough surfaces is

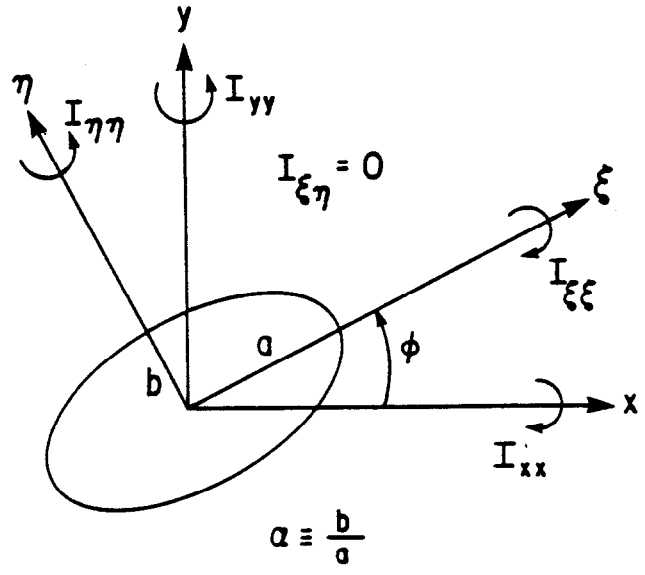

Fig. 8 Second moments of area for elliptical contact

$$\psi = \psi_\infty(\alpha,\mu)+\epsilon g(\beta)+\frac{\epsilon^3\beta^{3/2}}{4\pi^2}\left\{1.202\left[3\alpha\sin^2\phi+\frac{3}{\alpha}\cos^2\phi - \alpha-\frac{1}{\alpha}\right) + \frac{1}{\beta^3}\left(3\alpha\cos^2\phi + \frac{3}{\alpha}\sin^2\phi - \alpha - \frac{1}{\alpha}\right)\right] + 2\left(3\alpha\sin^2\phi + \frac{3}{\alpha}\cos^2\phi - \alpha - \frac{1}{\alpha}\right) f_1(\beta) + 6\left(2\alpha\cos^2\phi + \frac{2}{\alpha}\sin^2\phi - \alpha - \frac{1}{\alpha}\right) f_2(\beta)\right\} \quad (60)$$

where $\psi \equiv k\sqrt{A_c}\,R_c$, μ is the flux distribution parameter (μ=0 for uniform flux, μ=-1/2 for equivalent isothermal flux), $\alpha \equiv b/a$ is the aspect ratio of the ellipse, $\epsilon \equiv \sqrt{A_c/A_t}$ is the dimensionless relative contact size (square root of the area ratio), $\beta \equiv d/c$ is the aspect ratio of the nominally rectangular elemental heat flux tube, and ϕ is the contact orientation angle with respect to the principal axes of the contact distribution as shown in Fig. 2.

At first glance Eq. (60) combined with Eqs. (35), (36), (37), (51), (52),, and (53) appears extremely lengthy for an "analytical expression". However once having accepted that Eq. (60) is inconvenient for hand calculation, these expressions can be easily programmed and rapidly executed on even the smallest of microcomputers and many programmable calculators. Furthermore since the alternative to the Method of Infinite Images is most likely three-dimensional numerical analysis, the length of these approximate analytical expressions is quite acceptable.

COMPARISONS WITH PREVIOUS DATA

Ideally when an approximate expression for the solution to some problem is derived, it is desirable to compare the new expression with previous data for all anticipated values of the independent parameters. For the expression developed in this work there are five independent parameters which would make a thorough study exhaustive. However no such study will be undertaken because there is simply little previous data to compare with.

For the limiting case of a circular contact on a square flux tube (α=β=1), accurate data can be found [5,13]. From this data it is determined that Eq. (60) predicts values of the constriction parameter which are about -.5% in error for the uniform flux case and -1.2% in error for the equivalent isothermal flux case at ϵ=.5. For values of ϵ<.3 this error diminishes to virtually zero.

Some limited data for $\alpha < 1$, $\beta < 1$ and $\phi = 0$ is available from Sadhal [5] in the form of a double-infinite Fourier series. The most "severe" case reported is α=.25 and β=.5. Fig. 9 shows graphically the relative dimensions of this problem for $.1 \leq \epsilon \leq .5$. In Table 1 the constriction parameter calculated by Eq. (60) of this work, ψ_{NYD}, is compared with that of Sadhal, ψ_S, for both flux cases at α=.25 and β=.5. From these results at ϵ=.5 the approximate expression for the constriction parameter given by Eq. (60) is -10% in error for the uniform flux and -14% in error for the equivalent isothermal flux. This is remarkable since an underlying assumption in the approximate analysis was that the elliptical contact is much smaller than the rectangular tube or that the constriction parameter for such a situation is only a small perturbation of the half-space result. However as shown in Fig. 9, at ϵ=.5 the elliptical contact has dimensions nearly comparable to that of the rectangular flux tube.

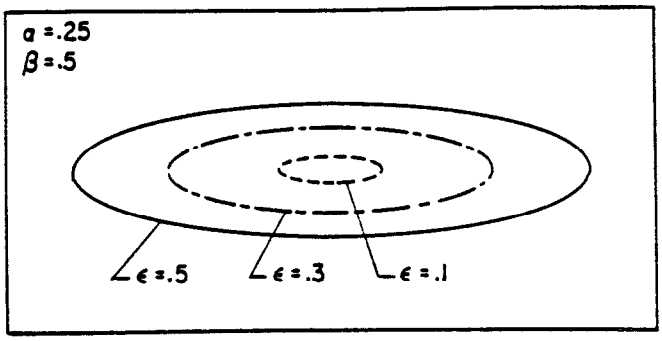

Fig. 9 Relative size of elliptical contact on rectangular flux tube for α=.25 and β=.5

	α=.25	β=.5	φ=0	
ε	μ = 0		μ = -1/2	
	ψ_S	ψ_{NYD}	ψ_S	ψ_{NYD}
.5	.148	.134	.119	.102
.4	.201	.195	.169	.163
.3	.256	.254	.224	.222
.2	.313	.312	.281	.280
.1	.370	.369	.338	.337

Table 1 Comparison of approximate constriction parameter given by Eq. (60) with exact data of Sadhal, ψ_S

As seen in Table 1, for $\epsilon \leq .3$ ψ_S and ψ_{NYD} are nearly identical. In addition for all other cases of $\alpha < 1$ and $\beta < 1$ reported by Sadhal, errors less than those of Table 1 were found for corresponding values of ϵ.

Since practical problems with anisotropic roughness can have much smaller values of β, comparison with data for $\beta \leq .1$ would be advantageous. However the actual criterion for the accuracy of Eq. (60) can really be determined by considering the accuracy of the Surface Element Method in predicting T_{ij} for the first row of image sources. With this consideration Eq. (60) can be expected to give adequate predictions of the constriction parameter of the elemental heat flux tube for anisotropic roughness because in most practical contact resistance problems ϵ will be less than .1.

CONCLUSIONS

From the expressions developed in this work, the constriction parameter for the elemental heat flux tube encountered with anisotropic roughness can be approximated accurately for small contact sizes as a perturbation of the half-space value. Useful approximate expressions for the two low-order perturbations have been generated by combining the techniques of the Surface Element Method and the Method of Infinite Images.

The first-order perturbation is given by the product of the relative contact size and a function

of the rectangular flux tube aspect ratio but is remarkably independent of the contact shape, orientation and boundary condition. Thus this term represents physically only an acknowledgement of the presence of four adiabatic walls instead of a half-space. An examination of this term shows that for a fixed small relative contact size, the constriction parameter increases as the elemental heat flux tube becomes more elongated. For a rectangle aspect ratio of $\beta < .14$ the constriction parameter of the elemental heat flux tube can actually be larger than that of a contact on a half-space. Both of these phenomena are logical since the net effect of continually decreasing the rectangle aspect ratio β is to approach the case of the strip contact source which has a larger resistance than that of the discrete elliptical contact.

However in practise anisotropic roughness will produce not only rectangular flux tube aspect ratios less than unity but also elliptical contact aspect ratios which are less than unity. Since the half-space resistance of an elliptical contact is lower than that of a circle, the leading term of the approximate expression for the constriction parameter is lower for the case of anisotropic roughness. Therefore depending on the exact geometry of the elemental heat flux tube, the contact resistance between anisotropic rough surfaces could be theoretically either higher or lower than that of the isotropic case for some given fraction of area in contact.

Although derived for a small relative contact size and/or a small perturbation of the half-space resistance, the approximate constriction parameter for the elemental heat flux tube has proven to be quite accurate even when the contact dimensions approach that of the flux tube and even when the flux tube constriction parameter is up to 70% lower than the half-space result. Thus because the relative contact sizes are usually very small for most practical problems involving anisotropic roughness, the approximate expressions developed in this work should be more than adequate. Furthermore since these simple expressions can be programmed into any small microcomputer, this approximation of the dimensionless thermal constriction resistance parameter represents a valuable tool for the ongoing theoretical and experimental investigation of the complex three-dimensional heat flow paths between real contacting surfaces.

ACKNOWLEDGEMENTS

The authors acknowledge the financial support of the Natural Sciences and Engineering Research Council under operating grant A7455 for Dr. Yovanovich and from a Postgraduate Scholarship for Mr. Negus.

REFERENCES

[1] Cooper, M., Mikic, B.B., and Yovanovich, M.M., "Thermal Contact Conductance", Int. J. of Heat and Mass Transfer, Vol. 12, Jan. 1969, pp. 279-300.

[2] Yovanovich, M.M., Hegazy, A., and Antonetti, V.W., "Experimental Verification of Contact Conductance Models Based Upon Distributed Surface Micro-Hardness", AIAA 21st Aerospace Sciences Meeting, Jan. 10-13, 1983, Reno, Nevada.

[3] DeChiffre, L., "Frequency Analysis of Surfaces Machined Using Different Lubricants," ASLE Transactions, Vol. 27, No.3, July 1984, pp. 220-226.

[4] Longuet-Higgins, M.S., "The Statistical Analysis of a Random Moving Surface," Phil. Trans. Royal Soc., Vol. A249, 1957, pp. 321-387.

[5] Sadhal, S.S., "Exact Solutions for the Steady and Unsteady Diffusion Problems for a Rectangular Prism", ASME Paper No. 84-HT-83, ASME 22nd Heat Transfer Conference, Niagara Falls, N.Y., Aug. 6-8, 1984.

[6] Beck, J.V., "Effects of Multiple Sources in the Contact Conductance Theory", ASME J. Of Heat Transfer, Vol. 101, Feb. 1979, pp. 132-136.

[7] Negus, K.J., and Yovanovich, M.M., "Constriction Resistance of Circular Flux Tubes with Mixed Boundary Conditions by Linear Superposition of Neumann Solutions", ASME Paper No. 84-HT-84, ASME 22nd Heat Transfer Conference, Niagara Falls, N.Y., Aug. 6-8, 1984.

[8] Yovanovich, M.M., Thompson, J.C., and Negus, K.J., "Thermal Resistance of Arbitrarily Shaped Contacts", Third International Conference on Numerical Methods in Thermal Problems, Seattle, Washington, Aug. 2-5, 1983.

[9] Grigull, U., and Sandner, H., Heat Conduction, Hemisphere, New York, 1984.

[10] Yovanovich, M.M., "Thermal Constriction Resistance of Contacts on a Half-Space: Integral Formulation", AIAA Progress in Astronautics and Aeronautics: Radiative Transfer and Thermal Control, Vol. 49, edited by A.M. Smith, New York, 1976, pp. 397-418.

[11] Meirovitch, L., Methods of Analytical Dynamics, McGraw-Hill, New York, 1980.

[12] Turyk, P.J., and Yovanovich, M.M., "Transient Constriction Resistance for Elemental Flux Channels Heated by Uniform Flux Sources", ASME Paper No. 84-HT-52, ASME 22nd Heat Transfer Conference, Niagara Falls, N.Y., Aug. 6-8, 1984.

[13] Negus, K.J. and Yovanovich, M.M., "Application of the Method of Optimised Images to Steady Three-Dimensional Conduction Problems", ASME Paper No. 84-WA/HT-110, ASME Winter Annual Meeting, New Orleans, Louisiana, Dec. 9-13, 1984.

[14] Yovanovich, M.M., Burde, S.S., and Thompson, J.C., "Thermal Constriction Resistance of Arbitrary Planar Contacts with Constant Flux", AIAA Progress in Astronautics: Theromophysics of Spacecraft and Outer Planet Entry Probes, Vol. 56, edited by A.M. Smith, New York, 1977, pp. 127-139.

[15] Chow, Y.L. and Yovanovich, M.M., "The Shape Factor of the Capacitance of a Conductor", J. of Applied Physics, Vol. 53, No. 12, Dec. 1982.

[16] Abramowitz, M., and Stegun, I.A., Handbook of Mathematical Functions, Dover, New York, 1972.

[17] Wolfe, P.J. and Meeter, "Non-Linear Least Squares (GAUSHAUS)", University of Wisconsin Computing Center, Dec. 1965.

[18] Yovanovich, M.M., ME 758 Course Notes, University of Waterloo, Jan. 1983.

[19] Yovanovich, M.M., Personal Communication, Jan. 1985.

[20] Gradshteyn, I.S. and Ryzhik, I.M., Table of Integrals, Series and Products, Academic Press, New York, 1980.

[21] Jahnke, E., and Emde, F., Tables of Functions, Dover, New York, 1945.

[22] Flugge, W., Handbook of Engineering Mechanics, 1962.

[23] Ramsey, A.S., Newtonian Attraction, Cambridge University Press, London, 1981.

APPENDIX I

Average Induced Temperature Rise of Planar Contacts with Uniform Flux

Consider two arbitrarily shaped planar contacts on the surface of an adiabatic half-space of thermal conductivity k as shown in Fig. 10. The average temperature rise over contact 1, $\bar{T}_1$, can be written by linear superposition of solutions to Laplace's equation as

$$\bar{T}_1 = \bar{T}_{11} + \bar{T}_{12} \tag{I-1}$$

where $\bar{T}_{11}$ represents the average temperature rise on contact 1 due to its own flux distribution acting alone on an adiabatic half-space and $\bar{T}_{12}$ is the average temperature rise induced on contact 1 due to the uniform flux q_2 prescribed over contact 2.

In this Appendix an approximate expression will be derived for $\bar{T}_{12}$. The derivation is an abbreviated version of that given in [8] which was originally motivated by work in Newtonian potential theory [23].

By linear superpostion of point sources, the temperature rise at some location P on contact 1 due to contact 2 is

$$T_P = \int_{A_2} \frac{q_2 dA_2}{2\pi k\rho} = \frac{q_2}{2\pi k} \int_{A_2} \frac{dA_2}{\rho} \tag{I-2}$$

By applying the Cosine Law then

$$\rho^2 = \rho_o^2 + r^2 - 2r\rho_o\cos\theta \tag{I-3}$$

$$T_P = \frac{q_2}{2\pi k} \int_{A_2} (\rho_o^2 + r^2 - 2r\rho_o\cos\theta)^{-1/2} dA_2 \tag{I-4}$$

Since in general $r < \rho_o$ the integral can be expanded by the Binomial Theorem to give

$$T_P = \frac{q_2}{2\pi k\rho_o} \int_{A_2} [1 - \frac{r^2}{2\rho_o^2} + \frac{r\cos\theta}{\rho_o} + \frac{3r^2\cos^2\theta}{2\rho_o^2} + \ldots] dA_2 \tag{I-5}$$

or if higher order terms are neglected

$$T_P = \frac{q_2}{2\pi k\rho_o} \{ \int_{A_2} dA_2 + \int_{A_2} r\cos\theta dA_2 + \int_{A_2} \frac{(2r^2 - 3r^2\sin^2\theta)}{2\rho_o^2} dA_2 \} \tag{I-6}$$

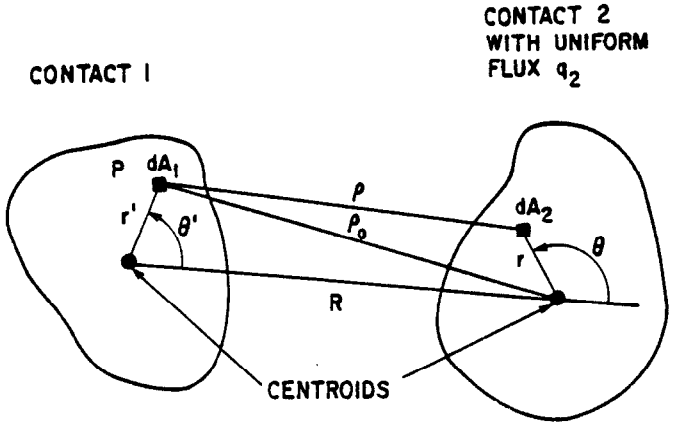

Fig. 10 Two arbitrary planar contact areas for derivation of the Surface Element Method

The first integral is simply the area A_2. The second integral vanishes identically by the definition of centroidal location. For the third integral recall that

$$I_o \equiv \int_A r^2 dA \tag{I-7}$$

$$I_{RR} \equiv \int_A r^2\sin^2\theta dA \tag{I-8}$$

where I_o is the polar second moment of area about the centroid (or "polar moment of inertia") and I_{RR} is the radial second moment of area about the axis ρ_o. Thus the temperature rise at some location P on contact 1 is approximately

$$T_P = \frac{q_2}{2\pi k} \{ \frac{A_2}{\rho_o} + \frac{2I_o^{(2)} - 3I_{RR}^{(2)}}{2\rho_o^3} \} \tag{I-9}$$

The average induced temperature rise on contact 1 is given by

$$\bar{T}_{12} = \frac{1}{A_1} \int_{A_1} T_P \, dA_1 = \frac{q_2}{2\pi k} \{ \frac{A_2}{A_1} \int_{A_1} \frac{dA_1}{\rho_o} + \frac{2I_o^{(2)} - 3I_{RR}^{(2)}}{2A_1} \int_{A_1} \frac{dA_1}{\rho_o^3} \} \tag{I-10}$$

Note that an assumption has been made that $I_{RR}^{(2)}$ is constant which is not strictly true for shapes that are not doubly-symmetric. However by using a value for $I_{RR}^{(2)}$ taken about the axis joining the centroids of the two contacts, the approximation is fairly accurate and improves as the contacts are located further apart.

The first integral can be treated as before by making the transformation

$$\rho_o^2 = R^2 + (r')^2 - 2Rr'\cos\theta' \tag{I-11}$$

Then after ignoring higher-order terms as before the integral becomes

$$\int_{A_1} \frac{dA_1}{\rho_o} = \frac{A_1}{R} + \frac{2I_o^{(1)} - 3I_{RR}^{(1)}}{2R^3} \tag{I-12}$$

where R is the distance between the two centroids as shown in Fig. 10.

The second integral is simply

$$\int_{A_1} \frac{dA_1}{\rho_o^3} = \frac{A_1}{R^3} \tag{I-13}$$

if higher order terms are neglected.

Thus an approximate expression for the average induced temperature rise on contact 1 due to an uniform flux q_2 on contact 2 is

$$\bar{T}_{12} = \frac{q_2}{2\pi k} \{ \frac{A_2}{R} + (\frac{A_2}{A_1}) \frac{2I_o^{(1)} - 3I_{RR}^{(1)}}{2R^3} + \frac{2I_o^{(2)} - 3I_{RR}^{(2)}}{2R^3} \} \tag{I-14}$$